


 Cite this: *RSC Adv.*, 2024, 14, 29413

Design and comprehensive characterization of dry powder inhalation aerosols of simvastatin DPPC/DPPG lung surfactant-mimic nanoparticles/microparticles for pulmonary nanomedicine

 David Encinas-Basurto,^{ab} Maria F. Acosta,^a Basanth Babu Eedara,^{id ac}
 Jeffrey R. Fineman,^d Stephen M. Black^{ce} and Heidi M. Mansour^{id *acef}

The Rho Kinase (ROCK) pathway is recognized to be involved in changes that lead to remodeling in pulmonary hypertension (PH), particularly cellular processes including signaling, contraction, migration, proliferation, differentiation, and apoptosis. Simvastatin (Sim) has a potent anti-proliferative and pro-apoptotic effect on vasculature smooth muscle cells through the inhibition of the synthesis of isoprenoids intermediates which are essential for the post-translational isoprenylation of Rho, Rac, and Ras family GTPases. Sim targets the underlying mechanism in vascular remodeling. Using bionanomaterials and particle engineering design, this innovative study reports on the advanced inhalable dry powders composed of sim with synthetic phospholipid bionanomaterials, DPPC/DPPG, as a lung surfactant-mimic. These were successfully designed and produced as co-spray dried (Co-SD) nanoparticles and microparticles for nanomedicine delivery as dry powder inhalers (DPIs). Different techniques were used to comprehensively characterize the physicochemical properties of the resulting Co-SD particles. The Next Generation Impactor™ (NGI™) was used with three different FDA-approved human DPI devices with varying shear stress which were the HandiHaler®, Neohaler®, Aerolizer® DPI devices for aerosol dispersion performance. The formulation–device interactions were examined and correlated. Using human lung cells from different lung regions, *in vitro* cell viability and transepithelial electrical resistance (TEER) at the air-liquid interface showed biocompatibility of the formulations as a function of dose.

 Received 9th July 2024
 Accepted 5th September 2024

DOI: 10.1039/d4ra04947k

rsc.li/rsc-advances

Introduction

Pulmonary hypertension (PH) is a lung condition characterized by elevated resting blood pressure (25 mm Hg or higher) in the pulmonary arteries.^{1–3} PH impairs the ability of the right ventricle of the heart to pump blood effectively. As a result, the imbalanced production of vasodilators and vasoconstrictors results in excessive vasoconstriction. Furthermore, remodeling of the vasculature occurs due to physiological and biochemical

changes such as inflammation and thrombosis (due to endothelial dysfunction and platelet aggregation), as well as endothelial and vascular smooth cell proliferation and inhibition of apoptosis.⁴

Due to the avoidance of first-pass metabolism and direct delivery to the treatment site, pulmonary drug delivery is the ideal treatment for PH.⁵ Other advantages include a faster onset of action, lower systemic exposure, fewer side effects, and the ability to overcome the challenges of poor gastrointestinal absorption.⁶ The FDA-approved inhalation products currently used clinically to treat PH by inhalation include Ventavis® (nebulized iloprost), Tyvaso® (nebulized treprostinil and dry powder inhaler), and INOmax® (inhaled nitric oxide gas). The disadvantage of nebulized liquid aerosols include high dosing administration frequency, which necessitates 6 to 9 nebulized liquid aerosol treatments per day, and relatively long treatment times per dose administration. Furthermore, there are several potential adverse drug effects, including an increased risk of bleeding for anticoagulant patients, bronchospasms, wheezing, and a drop in blood pressure resulting in dizziness. Ventavis® inhibits platelet aggregation; however, the significance of this

^aSkaggs Pharmaceutical Sciences Center, College of Pharmacy, The University of Arizona, AZ, USA

^bBiopolymers-CTAOA, Research Center for Food and Development (CIAD, A.C.), Hermosillo, Mexico

^cCenter for Translational Science, Florida International University, 11350 SW Village Parkway, Port St. Lucie, FL 34987-2352, USA. E-mail: hmansour@fiu.edu; Tel: +7(772) 345-4731

^dDepartment of Pediatrics, University of California San Francisco School of Medicine, San Francisco, CA, USA

^eDepartment of Medicine, Division of Translational and Regenerative Medicine, The University of Arizona College of Medicine, Tucson, AZ, USA

^fThe University of Arizona, BIO5 Institute, Tucson, AZ, USA



effect in the treatment of pulmonary hypertension is unknown.⁷ In addition, there is a lack of selectivity, which leads to off-target side effects and the need to target two or more pathways to slow the progression of PH. Most importantly, all current therapies aim to reverse symptoms rather than the underlying cause of the disease, thus limiting their therapeutic efficacy.⁸

Recent research has implicated the activation of the small G protein RhoA and its target Rho Kinase, also known as the Rho Kinase pathway, in some of the changes that lead to vasculature remodeling in PH, particularly cellular processes (including signaling, contraction, migration, proliferation, differentiation, and apoptosis)^{9,10} showed that simvastatin (Sim) affects post-translational isoprenylation of Rho, Rac, and Ras family GTPases by inhibiting the synthesis of isoprenoids intermediates. In addition, RhoA/ROCK inhibits endothelial function by expressing and activating eNOS.¹¹ Simvastatin to treat PH provided additional impetus to develop an advanced inhalable formulation that can be delivered to the respiratory tract as dry powder inhalers (DPIs) using an FDA-approved human DPI device.

In comparison to liquid aerosols, dry powder inhalers (DPIs) offer chemical and physical stability of molecules drugs due to their solid-state, the ability to include hydrophobic (water-insoluble) drugs, patient compliance, more versatile inhaler devices, fewer excipients, and the lack of need for propellant and hand-to-lung coordination.^{12–14}

Phospholipids are important bionanomaterials and certain phospholipids are essential components in normal lung surfactant composition and its function in the lungs. Lung surfactant exists a multilamellar (*i.e.* multinanolayers) structure and as a monolayer (*i.e.* a nanolayer) at the air–liquid interface. Synthetic phospholipids, dipalmitoylphosphatidylcholine (DPPC), a zwitterionic phospholipid essential in normal lung surfactant nanolayer and dipalmitoylphosphatidylglycerol (DPPG), as PG is also in lung surfactant, were rationally chosen as lung surfactant-mimic phospholipids and in a lung surfactant-relevant molar ratio of DPPC : DPPG 3 : 1 as a nano-carrier for Sim. They are the most common phospholipid components found in the lungs and are required for appropriate lung surfactant function.^{15,16} The thermodynamically stable multilamellar state of the resultant particles powder is formed,¹⁷ and unlike other inhaled particles, the destiny of these components is comparable to that of native lipids. The purpose of this innovative study is to design, develop, and comprehensively characterize simvastatin-loaded proliposomal co-spray dried (Co-SD) inhalable powders that target the RhoA/Rho kinase (ROCK) pathway as a potentially new nanomedicine treatment for pulmonary hypertension. In addition, this study reports on the *in vitro* aerosol dispersion performance of these innovative inhalable dry powder nanoformulations combined with three different types of FDA-approved unit-dose capsule-based DPI devices that differed in device shape, resistance, and shear stress properties. Biocompatibility with human lung cells was evaluated using *in vitro* cell viability and trans-epithelial electrical resistance (TEER) at the air–liquid interface. To the Authors' knowledge, this study is the first to report such findings using these conditions including the advanced spray

drying conditions, these synthetic phospholipids in the reported ratio, *in vitro* human cellular studies on multiple lung cell types, and aerosol dispersion performance using 3 different FDA-approved DPI devices.

Materials and methods

Materials

Simvastatin (Sim) [United States Pharmacopeia (USP) grade] was obtained from ACROS (New Jersey, USA). Methanol (HPLC grade, ACS-certified grade, purity 99.9%) was obtained from Fisher Scientific (Fair Lawn, New Jersey, USA). Hydranal[®]-Coulomat AD and resazurin sodium salt were purchased from Sigma-Aldrich (St. Louis, MO, USA). Raw and spray-dried Sim powders were stored in sealed glass desiccators with Drierite[™] desiccant/Drierite indicating desiccant at $-20\text{ }^{\circ}\text{C}$ under ambient pressure. Ultra-high purity (UHP) nitrogen gas (Cryogenics and gas facility, The University of Arizona, Tucson, Arizona) was used during advanced spray drying in closed-mode as the drying gas and atomizing gas. Synthetic DPPC (molecular weight $734.039\text{ g mol}^{-1}$, >99% purity) and DPPG (molecular weight $744.952\text{ g mol}^{-1}$, >99% purity) sodium salt were obtained from Avanti Polar Lipids (Alabaster, AL, USA).

Methods

Advanced spray-drying from organic solution. The Sim-loaded proliposome particles in the solid stated were designed by particle engineering design and production using advanced spray drying in closed-mode, using a similar method earlier reported by our group.^{18,19} DPPC and DPPG were dissolved in a ratio of 1 : 3 with varying amounts of Sim in methanol (no water) using solid final 0.1% (w/v) concentration in the feed solution following spray-dried by B-290 Büchi Mini Spray Dryer coupled with a B-295 Inert Loop and a High-Performance cyclone (Büchi Labortechnik AG, Switzerland) and using a stainless-steel nozzle diameter was 0.7 mm in closed-mode. The use of methanol and no water provides smaller droplet sizes due to the surface tension of methanol, in contrast to the high surface tension of water, and more efficient drying. The feed rate and the aspirator gas flow were set as 25%, 50%, and 100% and 35 m^3 per hour (90%). The drying air inlet temperatures were $150\text{ }^{\circ}\text{C}$. After spray drying, all SD powders were stored in glass vials sealed with parafilm in desiccators at $-20\text{ }^{\circ}\text{C}$ until further characterization. The spray drying conditions are summarized in Table 1.

Laser diffraction particle size and size distribution. The particles mean size and size distribution were determined by the nanosizer analyzer SALD-7101 (Shimadzu, Japan). The measured sample was prepared by dispersing 10 mg of dry powder (DP) proliposomes in 1 mL Milli Q water and sonicated for 5 minutes. The sample was added to the blank for measurement, and 1.60–0.10 refractive index was used. In addition to acquiring the particle size distributions, the D_{v10} , D_{v50} , and D_{v90} parameters were measured. The span value was calculated using the eqn (1):



Table 1 Co-spray-dried (co-SD) formulation solution (0.1% w/v) and their corresponding outlet temperatures during spray-drying ($n = 3$). PL: phospholipids. Sim: simvastatin

| Sample (Sim : PL) | % pump rate | Outlet temperature (°C) |
|-------------------|-------------|-------------------------|
| 25 : 75 | 25 | 52–54 |
| 25 : 75 | 50 | 60–63 |
| 25 : 75 | 100 | 40–42 |
| 50 : 50 | 25 | 60–64 |
| 50 : 50 | 50 | 57–60 |
| 50 : 50 | 100 | 38–41 |
| 75 : 25 | 25 | 54–57 |
| 75 : 25 | 50 | 58–61 |
| 75 : 25 | 100 | 45–48 |

Table 2 Volumetric particle sizes (D_{v10} , D_{v50} , and D_{v90}), of co-SD Sim : PL produced at the high (100%) pump rate ($n = 3$, mean \pm SD)

| Co-SD Sim : PL powders | D_{v10} (μm) | D_{v50} (μm) | D_{v90} (μm) | Span |
|------------------------|-----------------------------|-----------------------------|-----------------------------|-----------------|
| 25 : 75 | 0.175 \pm 0.04 | 0.385 \pm 0.08 | 1.05 \pm 0.04 | 2.27 \pm 0.05 |
| 50 : 50 | 0.199 \pm 0.06 | 0.408 \pm 0.09 | 1.12 \pm 0.03 | 2.25 \pm 0.04 |
| 75 : 25 | 0.288 \pm 0.04 | 0.620 \pm 0.12 | 1.35 \pm 0.07 | 1.71 \pm 0.06 |

$$\text{Span} = [(D_{v90} - D_{v10})/D_{v50}] \quad (1)$$

Karl Fisher titration

Using conditions similar to previously reported,²⁰ the residual water content of all co-SD powders were quantified analytically by Karl Fisher titration (KFT) using a TitroLine 750 trace titrator (SI Analytics, Weilheim, Germany). Approximately 5 mg of powder was added to the titration cell containing Hydranal® Coulomat AD reagent.

Scanning electron microscopy

A scanning electron microscopy (SEM) using a FEI Inspect S microscope (FEI, Brno, Czech republic) was used to observe the morphology and particle size of the dry powders. All the samples were fixed on an aluminum stub using double-sided adhesive tabs (TedPella, Inc. Redding CA) and then sputter-coated with gold prior to visualization with a Hummer 6.2 sputtering system from Anatech (Union City, CA) as previously reported.¹⁹ The accelerating voltage was set as 15.0 kV. Photo micrographs were taken at different magnifications in different regions of the sample.

X-ray powder diffraction

Powder crystallization was evaluated by X-ray diffraction (XRPD, D8, Quest Bruker Corporation, Bremen, Germany) and collected at room temperature with a PANalytical X'pert diffractometer (Westborough, MA, USA). Measurements were taken between 5.0° and 50.0° (2θ) with a scan rate of 2.00° per min at ambient

temperature. The powder samples were loaded on a zero-background silicon sample holder.²¹

Differential scanning calorimetry

Differential scanning calorimetry (DSC) was applied to investigate the thermal properties of the Co-SD proliposomes. Approx. 5–10 mg powder was placed into an anodized aluminum hermetic DSC pan. The TA Q1000 differential scanning calorimeter (DSC) (TA Instruments, New Castle, DE) was used for thermal analysis and phase transition measurements. The temperature range was from -5.00 °C to 300.00 °C with a heating scan rate of 5.00 °C min^{-1} under a continuous flow of nitrogen gas. All measurements were carried out in triplicate ($n = 3$).

Hot stage microscopy (HSM) under cross-polarizers

Dry proliposomes at 50 : 50 were fixed on a glass slide and heated using the same DSC conditions described earlier using a Leica DMLP cross-polarized microscope (Wetzlar, Germany) equipped with a Mettler FP 80 central processor heating unit and Mettler FP82 hot stage (Columbus, OH, USA).²⁰ The images were captured digitally with a Nikon coolpix 8800 digital camera (Nikon, Tokyo, Japan) at 10x optical zoom and 10x digital zoom.

Attenuated total reflectance-Fourier transform infrared spectroscopy (FTIR)

The FTIR spectra of Co-SD proliposomes, Sim, DPPC and DPPG were undertaken using a Nicolet Avatar 360 FTIR spectrometer (Varian Inc., CA). The spectra were recorded with attenuated total reflectance (ATR) accessory. Each spectrum was collected for 32 scans at a spectral resolution of 2 cm^{-1} over the wave-number range of 4000 – 400 cm^{-1} . A background spectrum was carried out before every sample under the same experimental conditions.^{6,22}

Simvastatin loading analysis by high-performance liquid chromatography (HPLC)

Co-SD particles were dissolved in methanol at 1 mg mL^{-1} and sonicated for 15 minutes. Filter sample and inject into HPLC. Sim% drug loading (DL) were calculated as follow:

$$\% \text{Drug loading} = \frac{\text{Actual mass of sim}}{\text{Mass of particles}} \times 100 \quad (2)$$

The Sim contents in the co-SD proliposomes powder formulations were analyzed using a modified HPLC method.²³ The HPLC system consisted of an LC compact system (Shimadzu, Tokyo, Japan) equipped with a binary pump, a UV detector, a column oven, and an autosampler. For Sim HPLC analysis, the column was a Luna C₁₈ column (5 mm, 250 mm \times 4.6 mm i.d.; 3 μm ; Phenomenex, CA, USA), operated 25 °C. The mobile phase consisted of 100 mM ammonium acetate buffer-acetonitrile (40 : 60% v/v) at a 1.0 mL min^{-1} flow rate, with the UV detector wavelength set at 242 nm. A 10 μL of sample solutions was injected into the analytical column.





Fig. 1 SEM micrographs of: (A). Raw Sim; (B) Co-SD 25 : 75; (C). Co-SD 50 : 50; and (D). Co-SD 75 : 25. Molar ratio Sim : PL.

Table 3 The residual water content Co-SD Simvastatin formulations ($n = 3$, mean \pm SD)

| Co-SD powders (spray drying pump rate) | % (w/w) |
|--|----------------|
| Sim : PL 25 : 75 (100% PR) | 2.88 \pm 0.1 |
| Sim : PL 50 : 50 (100% PR) | 1.35 \pm 0.3 |
| Sim : PL 75 : 25 (100% PR) | 1.50 \pm 0.5 |

In vitro aerosol dispersion performance

The aerosolization performance of all powders was evaluated using the next generation impactor (NGI) (Copley Scientific Ltd, Nottingham, UK) with a suitable customized rubber mouth-piece adaptor and a stainless steel induction throat, in accordance with United States Pharmacopeia (USP) Chapter <601> on aerosol specifications.²⁴ The aerosol performance experiments were designed using Design-Expert 8.0.7.1 software (Stat-Ease Corp., Minneapolis, MN) and Vcaps[®] capsules #3 (Quali-V[®]; Qualicaps, Madrid, Spain). Using type A/E glass fiber filters with

a diameter of 55 mm on all stages except on stage 1 which used a 75 mm diameter A/E glass fiber filter, the mass of powder deposited on each stage was measured using a gravimetric method (PALL Corporation, Port Washington, NY). About 10 mg of powder was contained in each clear capsule.

One inhalation-grade capsule was loaded at a time into one of three different FDA-approved unit-dose human DPI devices with varying resistance to flow. The DPI devices were the Handihaler[®] (Boehringer Ingelheim, Ingelheim, Germany), Neohaler[®] (Sunovion Pharmaceuticals Inc, Marlborough, MA, USA), and Aerolizer[®] (Novartis Pharma AG, Basel, Switzerland). In each experiment, three capsules were used under ambient conditions using similar conditions described previously by our workgroup.^{21,25} The fine particle dose (FPD) was defined as the dose deposited on NGI stages 2–7, fine particle fraction (FPF) (eqn (3)), respirable fraction (RF) (eqn (4)), and emitted dose (ED) (eqn (5)) were calculated using the equations:

$$\text{Respirable fraction (RF\%)} = \frac{\text{FPD}}{\text{Total deposited dose}} \times 100\% \quad (3)$$



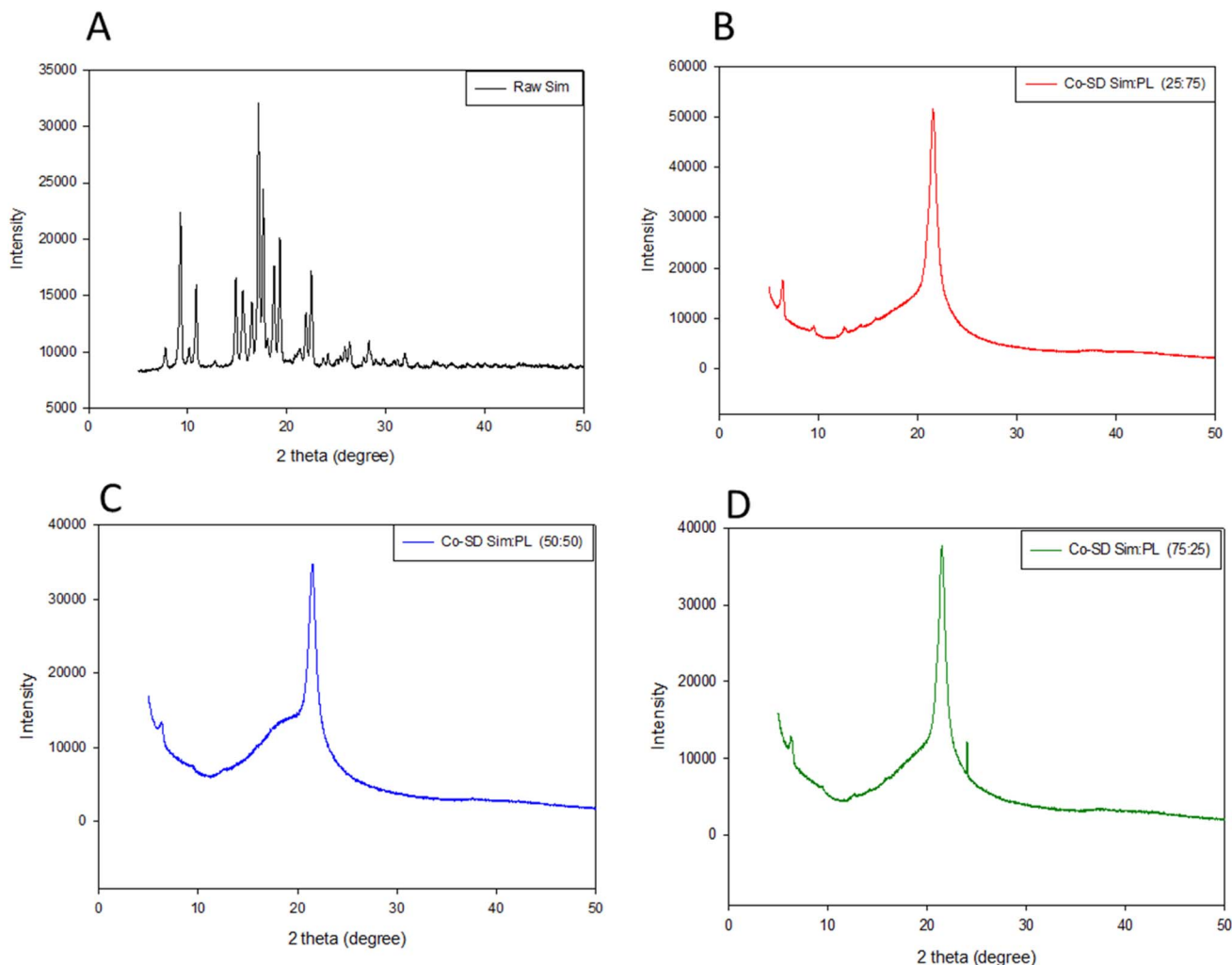


Fig. 2 X-ray powder diffractograms of raw Sim and co-SD DPPC/DPPG particles with varying Sim content. (A) Raw Sim; (B) Co-SD 75 : 25, Co-SD 50 : 50, Co-SD 25 : 75.

$$\text{Fine particle fraction(FPF\%)} = \frac{\text{FPD}}{\text{ED}} \times 100\% \quad (4)$$

$$\text{Emitted dose fraction(ED)} = \frac{\text{ED}}{\text{Total dose}} \times 100\% \quad (5)$$

In addition, the mass median aerodynamic diameter (MMAD) of aerosol particles and geometric standard deviation (GSD) were calculated using a Mathematica (Wolfram Research, Inc., Champaign, IL) program written by Dr Warren Finlay.²⁶

In vitro drug diffusion studies using the Franz cell

Modified Franz diffusion cell (VB6; PermeGear Inc., Hellertown, PA, USA) with Spectra/Por[®] membrane disc (12–14,000 MW) was used to assess the drug dissolution rate and diffusion of Sim-loaded proliposomes as previously reported with some modifications.^{27,28} Briefly, a volume of 5 mL of 0.02% Tween 20 PBS solution to facilitate Sim dissolution in aqueous solution was used in the acceptor media at a temperature of 37 ± 0.5 °C. A mass of 5 mg of Sim-loaded proliposome powder was

aerosolized by the Dry Powder Insufflator[™] device Model DP-4M (Penn-Century, Wyndmoor, PA) into the donor's vessel. At desired time points, 0.2 mL aliquots were removed with the replacement of new media. Each sample was analyzed by the modified HPLC method as described in detail below in the next section. All experiments were done in triplicate ($n = 3$).

In vitro human cell viability

A549 human lung alveolar cells and H441 human lung bronchioalveolar cells were obtained from ATCC (Manassas, VA, USA) and cultured in Dulbecco's modified Eagle's medium (DMEM) supplemented with 10% (v/v) fetal bovine serum (FBS), 100 IU mL⁻¹ of penicillin and 100 µg mL⁻¹ of streptomycin for A549 and RPMI 1640 with the same supplements for H441 were obtained from GIBCO by Life Technologies (Thermo Fisher Scientific Inc., Waltham, MA, USA). Cells were maintained in an incubator supplied with a 5% CO₂/95% air-humidified atmosphere at 37 °C. Cells were seeded at 5000 cells per well and 100 µL per well in 96-well plates, and after 48 hours, 100 µL per well of treatments with various Sim concentrations were added.



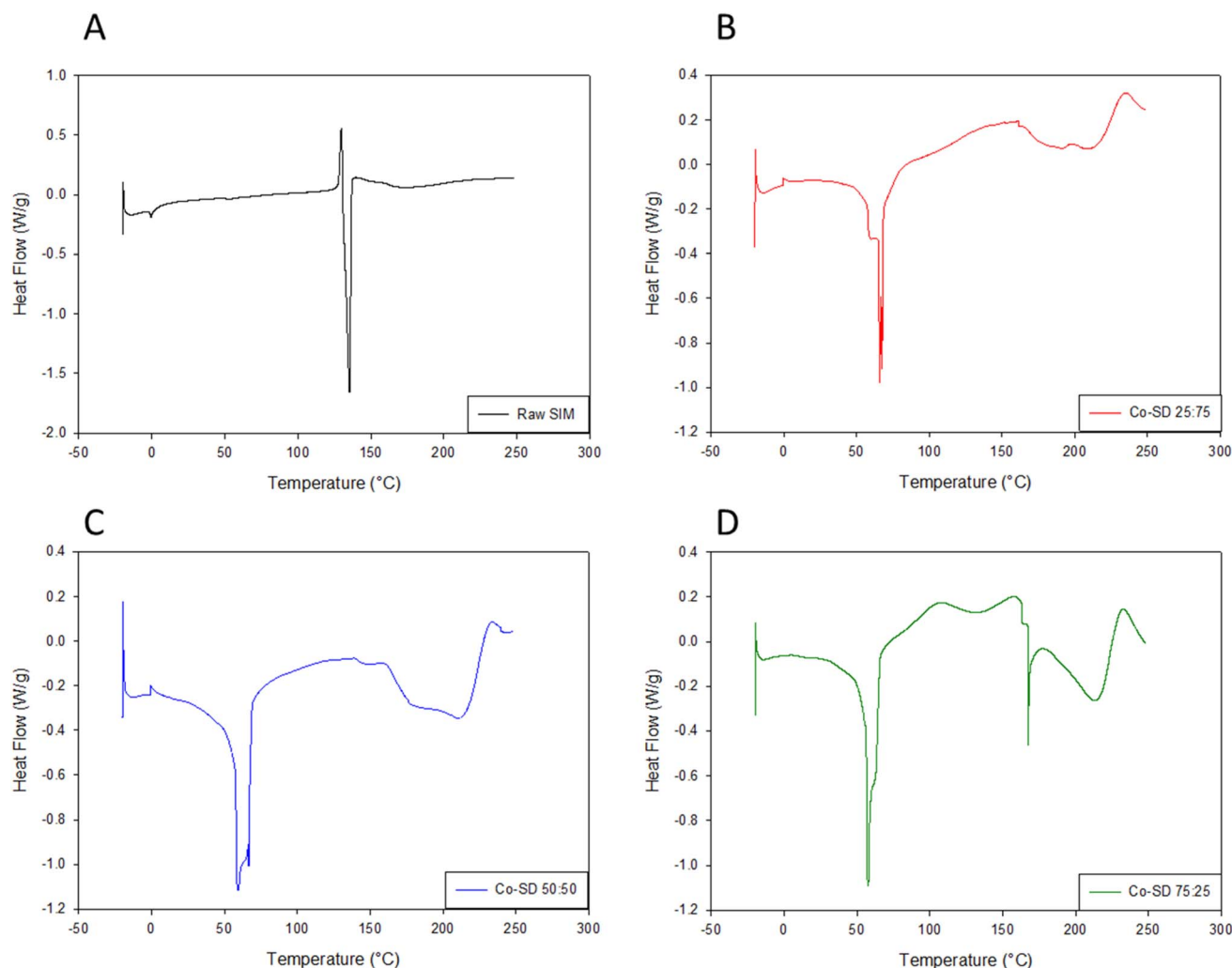


Fig. 3 Differential scanning calorimetry of raw Sim and co-SD DPPC/DPPG particles with varying Sim content. (A) Raw Sim; (B) Co-SD 25 : 75; (C) Co-SD 50 : 50; (D) Co-SD 75 : 25.

After 48 hours of exposure, each well was filled with 20 μL of 20 μM resazurin sodium salt and incubated for 4 hours. The fluorescence intensity of the resorufin (reduce state) produced by viable cells was detected using the Synergy H1 Multi-Mode

Reader at 544 nm (excitation) and 590 nm (emission) at this point (BioTek Instruments, Inc., Winooski, VT). The relative viability of each sample was calculated using eqn (6):

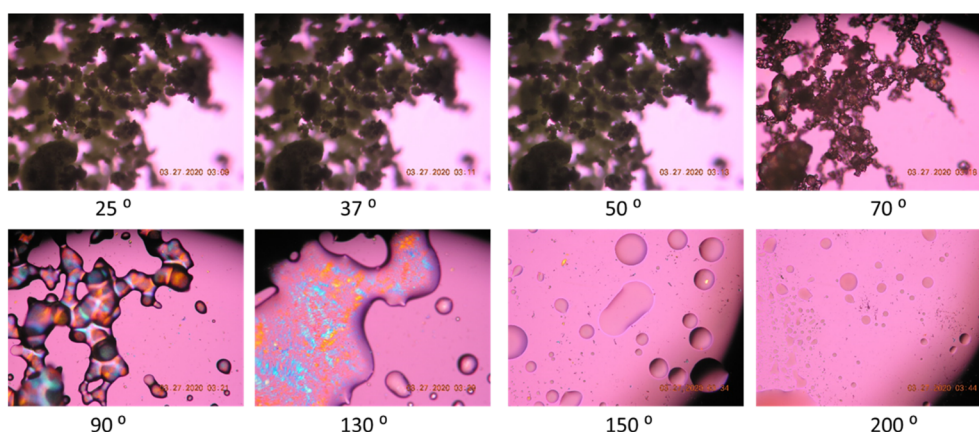


Fig. 4 Representative HSM images at different temperatures of Co-SD 50 : 50 Sim : PL.



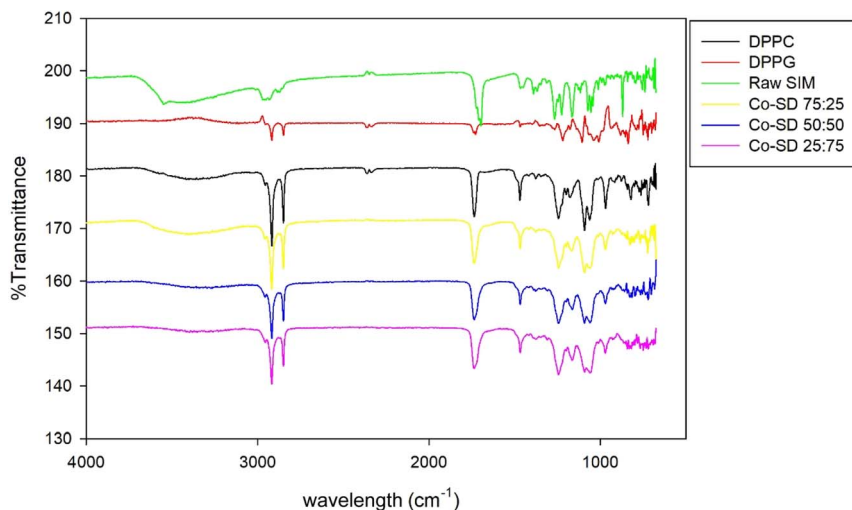


Fig. 5 ATR-FTIR spectra of raw Sim, DPPC, DPPG, Co-SD Sim : PL 25 : 75, Co-SD Sim : PL 50 : 50, and Co-SD Sim : PL 75 : 25 powders where PL is DPPC/DPPG.

Table 4 % Drug loading by HPLC for Co-SD Sim : PL powders where PL is DPPC/DPPG ($n = 3$, mean \pm SD)

| Formulation (Sim : PL) | % Drug loading |
|-------------------------|------------------|
| Co-SD 25 : 75 (100% PR) | 11.5 \pm 0.12 |
| Co-SD 50 : 50 (100% PR) | 17.8 \pm 0.095 |
| Co-SD 75 : 25 (100% PR) | 20 \pm 0.62 |

$$\text{Cell viability} = \frac{\text{Sample fluorescence intensity}}{\text{Control fluorescence intensity}} \times 100 \quad (6)$$

In vitro transepithelial electrical resistance (TEER)

TEER measurements were performed at the air-liquid interface (ALI) on H441 cells, as previously reported with some modifications.^{22,29} H441 cells were grown in T-75 culture flasks in an atmosphere of 5% CO₂ at 37 °C. H441 cells were maintained in

proliferation medium (RPMI 1640-Gibco) containing 10% fetal bovine serum (FBS), 1% PenStrep and 1% of GlutaMAX. Once they were confluent (90%), cells were seeded onto 12-well Transwell inserts[®] from Fisher Scientific (Hampton, New Hampshire) at a density of 500 000 cells per well in proliferation medium (0.5 mL in the apical and 1.5 mL in the basolateral chambers). After observing a complete monolayer under the microscope formed after 3–4 days, the apical side media was removed and every other day, the basolateral media was changed for the next days 5 days before changing to polarized media (RPMI 1640 containing 4% FBS, 1% penicillin-streptomycin, 1% GlutaMAX, 1% insulin-transferrin-selenium, and 200 nM dexamethasone). The polarized media was changed every next day. The maximum expected TEER at the ALI value was $\sim 250 \Omega \text{ cm}^{-2}$. Once they reached that value, cells were exposed to the 50 : 50 formulation for 3 hours, washed 3 times, and air-liquid interphase (ALI) condition was induced again. TEER monolayer recovery value was monitored for 5 days

Table 5 *In vitro* aerosol dispersion performance parameters of mass median aerodynamic diameter (MMAD), geometric standard deviation (GSD), fine particle fraction (FPF), respirable fraction (RF), and emitted dose (ED) for co-SD powders ($n = 3$, mean \pm SD)

| Co-SD Sim : PL powder composition | ED (%) | FPF (%) | RF (%) | MMAD (μm) | GSD |
|-----------------------------------|------------------|------------------|------------------|------------------------|------------------|
| HandiHaler[®] | | | | | |
| 25 : 75 | 100 \pm 0.02 | 32.72 \pm 2.49 | 56.01 \pm 4.96 | 4.04 \pm 0.33 | 1.99 \pm 0.84 |
| 50 : 50 | 99.9 \pm 0.04 | 15.99 \pm 1.60 | 28.1 \pm 0.68 | 11.84 \pm 1.87 | 2.78 \pm 0.32 |
| 75 : 25 | 99.7 \pm 0.34 | 13.84 \pm 2.46 | 30.45 \pm 1.62 | 10.77 \pm 1.03 | 2.89 \pm 0.07 |
| NeoHaler[®] | | | | | |
| 25 : 75 | 99.97 \pm 0.04 | 48.49 \pm 1.48 | 82.68 \pm 3.67 | 3.50 \pm 0.19 | 1.85 \pm 0.07 |
| 50 : 50 | 99.86 \pm 0.18 | 27.36 \pm 1.04 | 67.08 \pm 3.10 | 5.42 \pm 0.13 | 2.32 \pm 0.35 |
| 75 : 25 | 99.76 \pm 0.32 | 32.84 \pm 3.39 | 65.26 \pm 7.3 | 5.11 \pm 0.56 | 2.57 \pm 0.44 |
| Aerolizer[®] | | | | | |
| 25 : 75 | 99.7 \pm 0.26 | 62.55 \pm 2.77 | 87.87 \pm 4.1 | 3.14 \pm 0.16 | 1.86 \pm 0.056 |
| 50 : 50 | 92.9 \pm 8.77 | 27.65 \pm 3.34 | 59.25 \pm 4.06 | 4.48 \pm 0.15 | 2.25 \pm 0.07 |
| 75 : 25 | 99.36 \pm 0.89 | 28.80 \pm 0.81 | 71.304 | 4.18 \pm 0.14 | 2.03 \pm 0.09 |



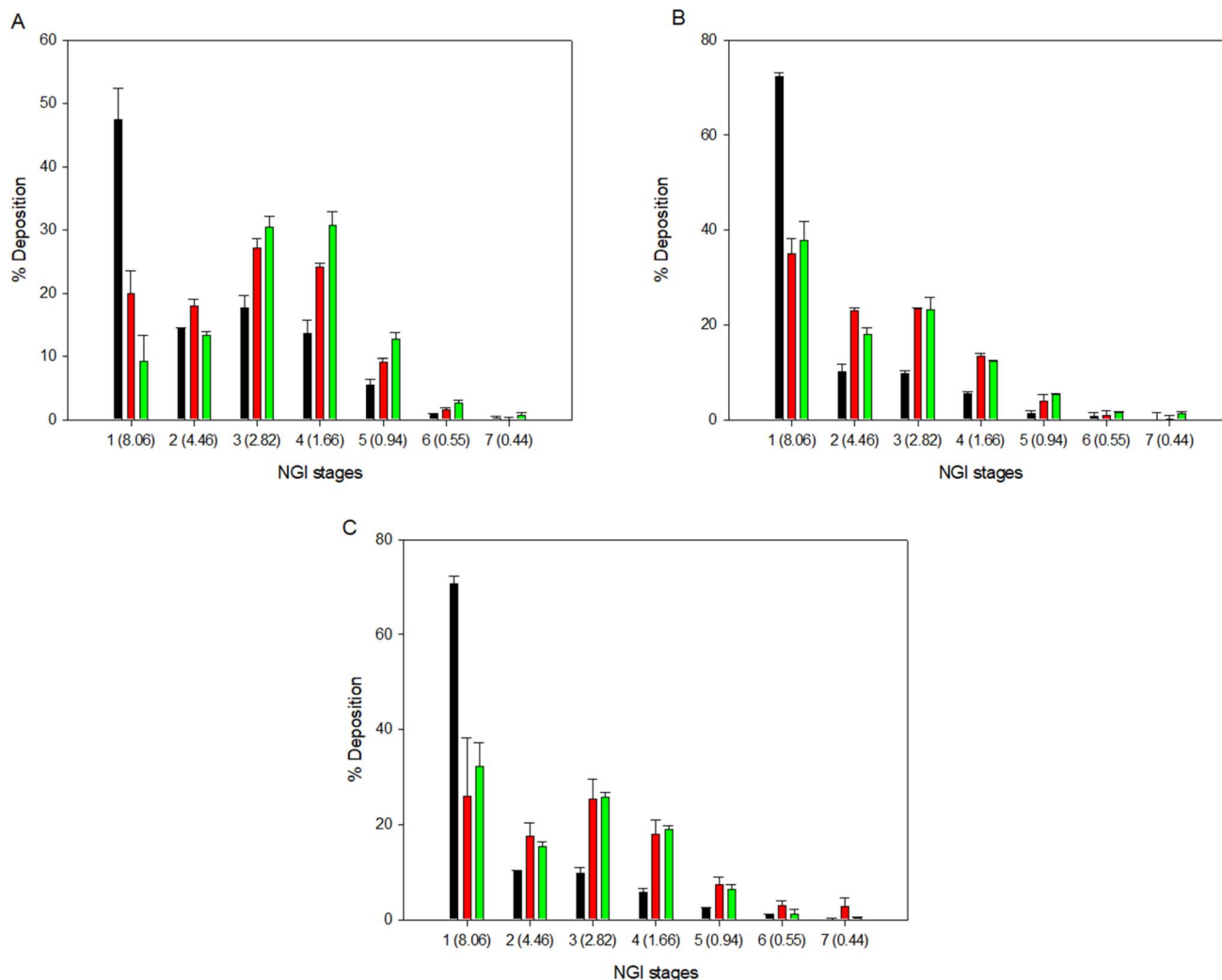


Fig. 6 *In vitro* aerosol dispersion performance as percent deposited on each stage of the Next Generation Impactor™ (NGI™) using NeoHaler® (red bars), HandiHaler® (black bars) and Aerolizer® (green bars) device for co-SD Sim : PL particles where PL is DPPC/DPPG: (A). 25 : 75 Sim : PL molar ratio; (B). 50 : 50 Sim : PL molar ratio; and (C). 75 : 25 Sim : PL molar ratio. $Q = 60 \text{ L min}^{-1}$ ($n = 3$, mean \pm SD).

using an EndOhm 12 mm Culture Cup (World Precision Instruments, Sarasota, FL, USA).

Statistical analysis

For Co-SD Sim *in vitro* aerosol testing, a multi-factorial design was used. The analysis of variance (ANOVA) test was performed with Design-Expert® 8.0.7.1 software (Stat-Ease Corp., Minneapolis, MN) was used to assess the interaction of the inhaler device resistance and molar ratio. 3D surface plots were generated by Design-Expert® 8.0.7.1 software (Stat-Ease Corp., Minneapolis, MN) to assess the effects of different interactions on the formulations' performance. All experiments ($n = 3$) were carried out in triplicate.

Results

Laser diffraction particle size and size distribution

As shown in Table 2, all Co-SD powders of Sim : PL (25 : 75, 50 : 50, 75 : 25) showed narrow and unimodal particle size distributions from the Span value observed (<2.5). It can be observed

that increasing Sim to the solution increased in volumetric particle size. It was clearly seen that the smallest particles are with the co-SD Sim : PL 25 : 75 powder with particle size range from 0.175 to 1.05 μm .

Morphology, shape, and size analysis

Particle morphology, surface morphology, and particle size were visualized *via* scanning electron microscopy (SEM). Fig. 1 shows the SEM micrographs of raw Sim and co-SD Sim-loaded proliposome prepared at three different molar ratios of Sim : PL at high spray drying pump rate (100%). Raw Sim (Fig. 1A) appears as long crystal structure, in good agreement with our earlier observation.²⁵ Compared with raw Sim, all co-SD Sim : DPPC/DPPG powders showed a significant particle size reduction, particle shape change, and surface morphology change.

Karl Fischer coulometric titration

The % residual water content in the Co-SD particles are shown in Table 3. The highest residual water content is found for the 25 :





Fig. 7 *In vitro* simvastatin release from co-SD Sim-loaded DPPC/DPPG particles in PBS medium at 37 °C: (A). Over 72 hours; and (B). First 2 hours. Molar ratio (Sim : PL) ($n = 3$, mean \pm SD).

75 molar ratio at 100% PR. It can be observed that by reducing DPPC content in the formulation, the percent residual water content decreased, resulting in the lowest residual water in the 50 : 50 formulation with $1.35 \pm 0.3\%$.

X-ray powder diffraction

X-ray powder diffraction (XRPD) diffractograms (Fig. 2) showed the presence of many sharp strong peaks which is due to the long-range molecular order in the crystalline powder of raw Sim (Fig. 2A) in good agreement with our earlier finding.²⁵ The co-SD Sim : PL 25 : 75, co-SD Sim : PL 50 : 50, and co-SD Sim : PL 75 : 25 powders, all exhibit the characteristic strong peak at $21^\circ 2\theta$, which corresponds to the presence of the phospholipid bilayer

structure.⁶ In addition, the intensity of the peak at $21^\circ 2\theta$ decreased with increasing Sim content for the formulated particles. The presence of many sharp peaks in raw Sim indicated that it was initially crystalline, however, upon spray-drying the bilayer-peak is present due to the influence of the DPPC/DPPG bilayer, and some Sim peaks were decreased indicative of amorphous drug character miscibility with the phospholipid bilayer.

Differential scanning calorimetry

DSC thermograms for formulated particles and their corresponding raw counterparts can be seen in Fig. 3. All formulation thermograms exhibited a characteristic bilayer main phase transition phase to the liquid crystalline phase, T_m , at $\sim 72^\circ \text{C}$,



Fig. 8 *In vitro* cell viability of 2 different human lung cell lines following dosing Co-SD proliposomes of varying Sim concentrations after 48 hours exposure at 37 °C for: (A). H441; and (B). A549 cells ($n = 3$, Mean \pm SD).



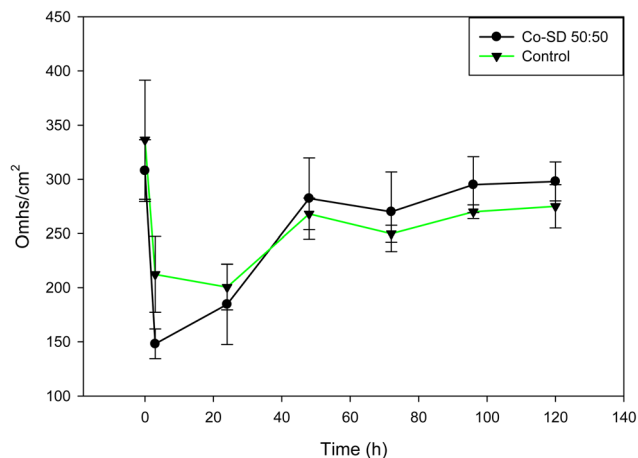


Fig. 9 Trans epithelial electrical resistance (TEER) of H441 lung epithelial cell exposed to Co-SD DPPC/DPPG particles (50 : 50) in air-liquid interface (ALI) culture conditions at 37 °C ($n = 3$, mean \pm SD).

confirming the miscibility of DPPC with DPPG.¹⁹ Raw Sim showed a small exotherm around 120 °C before the major endotherm, with the major endotherm around 135 °C. All liposomes systems underwent decomposition around 220 °C.

Hot stage microscopy (HSM) under cross-polarizers

Representative HSM micrographs of co-SD Sim : PL 50 : 50 particles are shown in Fig. 4. The sample initially showed dark agglomerates lacking visible birefringence until melting when some birefringence was visible which is the liquid crystalline characteristic of the DPPC/DPPG phospholipids. This is in good agreement with the XPRD diffractograms and DSC thermograms.

Attenuated total reflectance-Fourier-transform infrared spectroscopy (ATR-FTIR)

Formulated particles and their raw counterparts underwent ATR-FTIR analysis to determine the functional groups present in the system, as shown in Fig. 5. Many of the characteristic

peaks of raw DPPG were visible in the SD formulated particles, although their intensities decreased with increasing Sim content. In particular, strong peaks were present due to $-\text{CH}_2$ antisymmetrical stretching (2924 cm^{-1}), $-\text{CH}_3$ symmetrical stretching (2870 cm^{-1}), $\text{C}=\text{O}$ ester stretching ($1720\text{--}1735 \text{ cm}^{-1}$). The FT-IR spectra of pure Sim presented a characteristic peak at 1730 cm^{-1} ($\text{C}=\text{O}$ stretching) and 2960 cm^{-1} ($\text{C}-\text{H}$ stretch vibration).

Simvastatin drug loading analysis by HPLC

The formulated co-SD particles were analyzed for the Sim loading analyzed by HPLC. As listed in Table 4, the values were $11.5 \pm 0.12\%$, $17.8 \pm 0.095\%$, and $20 \pm 0.62\%$ for co-SD Sim : PL 25 : 75, co-SD Sim : PL 50 : 50, and co-SD Sim : PL 75 : 25 molar ratios, respectively.

In vitro aerosol dispersion performance

The aerosol properties of the formulated co-SD particles were evaluated using an NGI™ coupled with a different-resistance DPI device, and %ED, %FPF, %RF, MMAD and GSM parameters of each device are listed in Table 5. There was no significant difference in ED parameters using different DPIs ($p > 0.05$). In terms of the FPF, it can be observed that using 75 : 25 molar ratio formulation, FPF values are higher than the other ratios for all the DPIs used, having the highest using Aerolizer® DPI with 52.55 ± 2.77 . Regarding the RF, the higher value was observed for the 25 : 75 molar ratio and there was a clear difference between the DPIs used, finding better values when low-resistance DPI Aerolizer® was used. MMAD values increased with increasing Sim content in the feed solution, as seen in Table 5 observing values range from 3 to 11 μm . There were significant differences ($p < 0.05$) on MMAD values using different DPIs for each different molar ratio formulation.

The % deposition of the particles on each NGI™ stage is shown in Fig. 6 to show the aerosol dispersion performance of the formulated dry powder aerosols. All co-SD powders readily aerosolized with all 3 DPI devices. Aerosol deposition was detectable on all stages. The HandiHaler® DPI displayed a higher

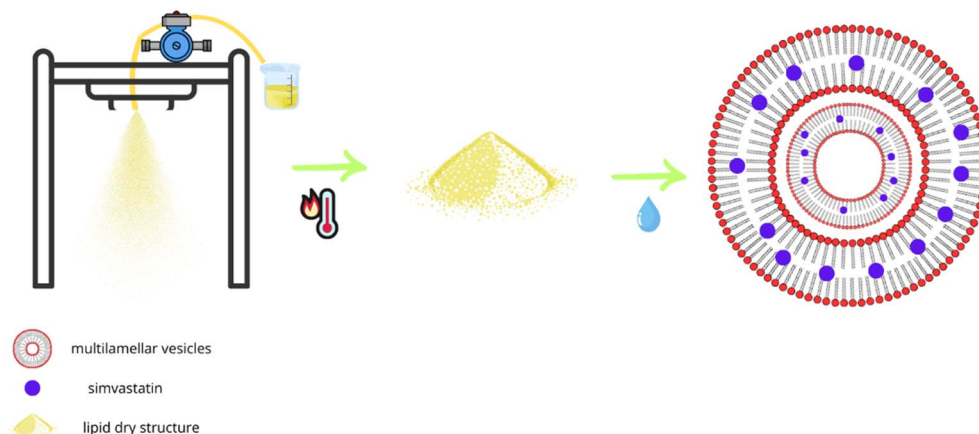


Fig. 10 Schematic illustration of simvastatin encapsulation *via* spray drying. Upon hydration, these particles form multilamellar vesicles (liposomes) with hydrophobic simvastatin encapsulated within the lipid bilayers.



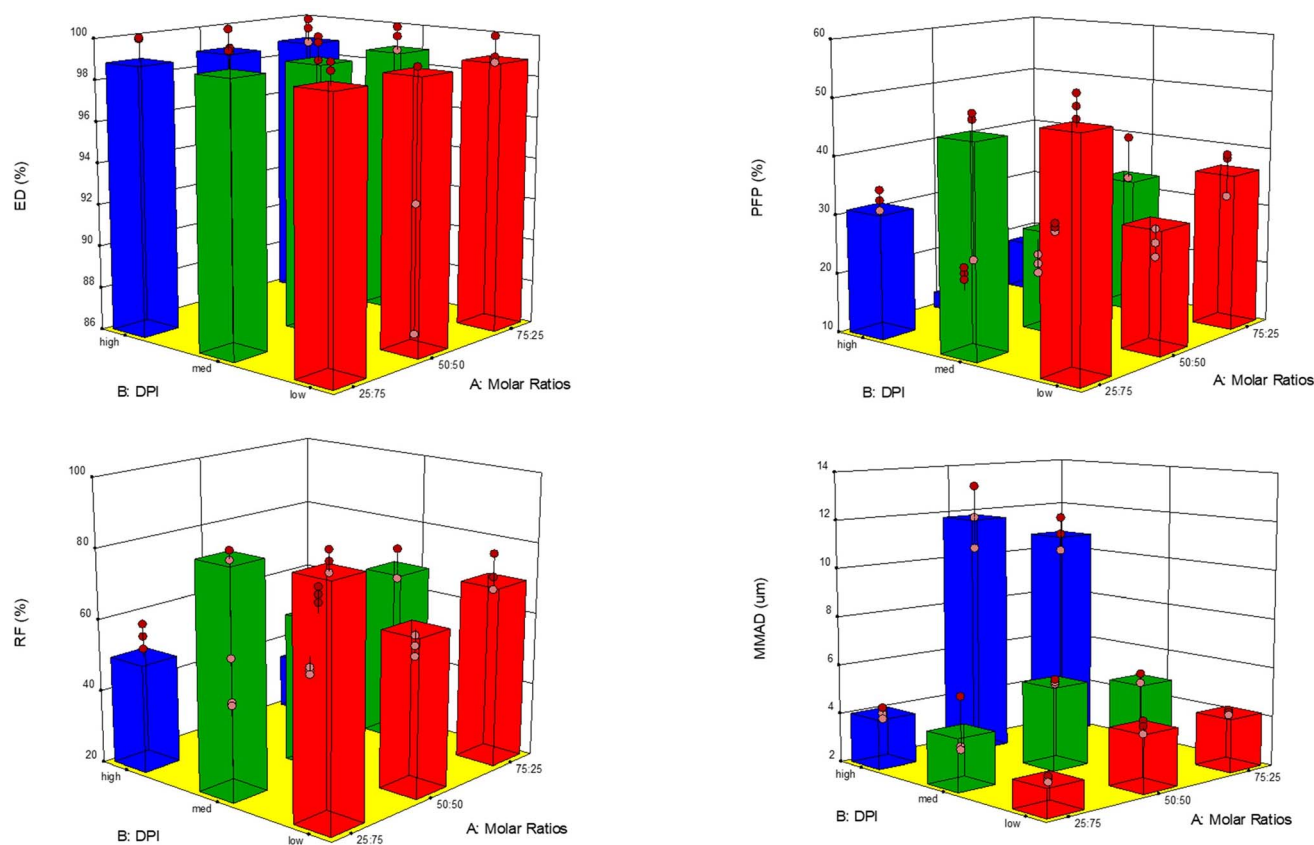


Fig. 11 3-D surface response plots showing the influence of the molar ratio in feed solution and inhalation device using the HandiHaler[®], NeoHaler[®], and Aerolizer[®] DPI device on *in vitro* aerosol dispersion performance for Co-SD Sim formulations for (A) ED; (B) PFP; (C) RF; (D) MMAD.

percent deposition at the more significant cut off diameter (8.06 µm) for all formulations. On the other hand, the NeoHaler[®] and Aerolizer[®] DPIs exhibited the highest percent deposition at lower cut-off diameters (2.82–1.66 µm) in stages 3 and 4 of the NGI. The results in Table 5 and Fig. 6 indicate that the DPIs used and the Sim content affected the aerosolization performance of proliposomes.

In vitro release studies of sim from DPPC/DPPG particles

In vitro release of Sim was evaluated with the particles suspended in a modified PBS medium. As shown in Fig. 7, a slow burst release for all formulations (Fig. 7B) can be observed, less than 3.5% for all formulations. After 3 days, 50%, 38%, and 36% of the Sim were released from the co-SD Sim : PL 25 : 75, 50 : 50, and 75 : 25 particles, respectively. The molar ratio of DPPC/DPPG on the Sim release profile starts to increase after 2 hours. The presence of DPPC led to an increase in the amount of Sim released after 24 hours to 32.5% for co-SD Sim : PL 25 : 75. However in contrast to the co-SD Sim : PL 50 : 50 and 75 : 25 systems, the amount of Sim released after 24 hours were 27.5% and 17.89%, respectively.

In vitro human cell viability

Fig. 8 shows the dose–response of different types of human lung cells after 48 hours of exposure to different doses of the

different formulations containing increasing amounts of Sim. Formulations tested were shown to be safe at concentrations of 1 µM, 10 µM, and 100 µM for A549 and up to 1000 µM to H441. There was no statistically significant difference between the non-treated cells and the cells treated with 1 µM, 10 µM, and 100 µM in both cell lines ($p > 0.05$). The relative viability of the cells decreased at 1000 µM concentrations, resulting in a statistically significant difference between the relative viability of the control cells (no treatment) and the relative viability of the cells exposed to the various formulations ($p < 0.05$) for the A549 cell line.

In vitro transepithelial electrical resistance (TEER) analysis upon particle exposure to lung epithelial cells

TEER measurements were completed on H441 cells to determine the effect of Sim-loaded formulated proliposomes on cells exposed to air-interface culture (AIC) conditions. Steady TEER values confirmed the presence of an effective cell monolayer (at least 300 Ω cm²) after 7 days of culturing under air-liquid interface (ALI) culture conditions and the presence of a cell monolayer *via* light microscopy (data not shown). The monolayer was exposed for 24 hours to the 50 : 50 formulation, the particles were washed out and TEER values started to be monitored for 5 days. After treatment, TEER values decreased significantly and as seen in Fig. 9, TEER values have



a recovering after 120 hours of treatment. The loss of electrical resistance and recovery suggests a reversible process, which ensures the integrity of the membrane barrier after particle deposition and indicates biocompatibility with cells. This is in good agreement with the *in vitro* cell viability data.

Discussion

When proliposomes come into touch with an aqueous surface, they create a closed lipid bilayer (multilamellar vesicles), acting as the provescicular precursor to liposomes.³⁰ Proliposomes, being a dry phospholipid formulation, provide more stability than liquid liposome dispersions, which may undergo hydrolysis, oxidation, sedimentation, fusion, or aggregation while being stored.³¹ The two main phospholipid components of lung surfactant, DPPC and DPPG, have transition temperatures above body temperature, which makes regulated drug release kinetics easier to achieve in drug delivery systems.^{6,17} Proliposomes are thermodynamically stable multilamellar liposomes in their solid state, are produced by co-spraying the drug with phospholipids using the spray drying procedure. In a spray dryer, the ethanolic solution mixture is atomized into fine droplets, and the drug is encapsulated by the phospholipids that self-assemble into proliposome particles due to rapid solvent evaporation. When these proliposome particles get humidity, they absorb water and become liposomes, which are multilamellar vesicles that form naturally. Sim undergoes this process whereby its hydrophobic parts merge with the lipid bilayers and its hydrophilic parts become trapped in the aqueous cores or inter-lamellar spaces (Fig. 10).

The physicochemical and *in vitro* aerosol performance properties of rationally formulated co-SD Sim-loaded proliposomes dry powders for pulmonary delivery were investigated in this study. Size distribution of described particles in the formulations allow for effective deep lung deposition while also providing enhanced stability during storage, and better solubility. Also, it was reported that micronized surfactant-based DPIs offer advantages over other systems as liquid aerosolized liposomes.^{6,18,32} Recent work by Barbălată *et al.* (2023)³³ reported on encapsulation of Sim using DPPC, egg PC, and cholesterol by thin-film hydration techniques followed by a spray drying process in open-mode from aqueous solutions of mannitol and leucine under different spray drying conditions from this study. The study reported here first advanced spray dried under different spray drying conditions in closed-mode without water to molecular mix Sim with synthetic DPPC/DPPG phospholipids in the lung surfactant ratio without any other excipients. This resulted in proliposome formulations optimized for aerosol performance and stability. Our study used synthetic DPPC/DPPG phospholipids and in the ratio that mimics lung surfactant, enhancing compatibility and performance for pulmonary delivery.

Three different Sim concentrations were tested (25, 50, and 75 in molar ratio to PL) in a systematic experimental design for DP optimization. The study elucidates the effect that Sim has on the Co-SD proliposomes and how it affects aerosol properties after aerosolization with different FDA-approved human DPIs

are used. As we have described previously, dilute organic alcohol feed solution (0.1% w/v feed concentration) results in smaller primary droplet sizes than aqueous solutions due to the lower surface tension of the alcohol in comparison to water. In addition, spraying from alcohols, which are regarded as “green chemicals”, promotes having a dryer powder. As a result, improved aerosol dispersion performance and stability due to this method eliminating water in the feed solution leading less residual water content in the final powder formulation.

The presence of the characteristic lipid bilayer structure when DPPC/DPPG phospholipids are present were evidenced by the XRPD peaks at 2θ and DSC thermogram showed characteristic bilayer phase transition (around 50 °C as our research group has reported previously^{6,18} for all formulations. In our work by Meenach *et al.*, (2014),¹⁹ the characteristic XRPD peak at $21^\circ 2\theta$ that indicated the presence of the lipid bilayer and the intensity of this peak decreased with increasing drug content. The DPPG diffractogram showed the presence of sharp peaks at 20 and $22.5^\circ 2\theta$, but not in the formulated particles and the presence of a strong peak at $21^\circ 2\theta$ for raw DPPC and for the raw materials, DPPC exhibited a crystal-to-gel (Tc) bilayer phase transition around 50.1 °C. This results are consistent to this work, where we can observe the DPPC peak at $21^\circ 2\theta$ and few remaining peaks from Sim in the 75 : 25 formulation and phase transitions of PL on the thermogram plots.

HPLC was used to analyze % DL resulting in effective encapsulation and confirming the presence of Sim within the phospholipid nanocarriers. The highest Sim content was in the 75 : 25 molar ratio with $20 \pm 0.62\%$ using 100% PR. This high payload in the powder will help in the need for a decrease in dose for an effective treatment against PH. Recently, treprostinil DPI was been approved for PH patients with PH and dry powder inhaler formulation LIQ861 (Liquidia, Inc.) significant fulfill benefits of this drug by delivering it to the lungs in 1 to 2 breaths compared to the nebulized solution that it needs up to 9 breaths to have the same dose.³⁴ This result confirms the importance of drug delivery by inhalation of dry powders to get higher doses of API.

Excellent *in vitro* aerosol dispersion performance was demonstrated using the NGI™ coupled with FDA-approved DPI devices. The results indicated that the formulated particles would be optimal for predominant deposition into the deep lung region for the Sim-loaded formulations. The formulations aerosolized with 3 different DPI devices showed excellent aerosol dispersion parameters that predict deposition in the middle and deep lung regions which is by sedimentation (gravitational settling) deposition mechanism.³⁵ Furthermore, the presence of DPPG and DPPG in the particle formulations enhanced the aerosol performance from previous work in our group of a Sim SD only, particular regarding the FPF and MMAD values which increased from a range of 24–41% without DPPG to 32–62% and for MMAD values of 5.1–19 μm^{25} without DPPC/DPPG to 3.1–11 μm for the current particle systems. In another previous work from our group,¹⁸ produced proliposomes using DPPC/DPPG system by Co-SD with the hydrophobic drug having similar aerosolization performance.



One-way analysis was performed using Design Expert[®] for individual and interaction of DPIs and formulation effect on % particle deposition in the different NGI stages. 3-D surface response plots were generated for all formulations (Fig. 11). DPI used and molar ratio tested showed statistical difference ($p < 0.0001$) for FPF, RF and MMAD parameters, only for ED didn't show any statistical difference as we values are very high for all DPIs tested (Table 5). For all co-SD formulations, the Neohaler[®] and Aerolizer[®] DPI devices gave the highest FPF and RF values compared to the Handihaler[®] device.

Sim release profiles from the phospholipid matrix vary significantly depending on the drug-to-phospholipid molar ratio, with higher Sim levels resulting in faster release. This faster release at higher drug loads (75 : 25 ratio) can be given to many causes. First, increasing Sim may disturb the PL matrix, resulting in broader diffusion routes and reduced matrix density, allowing for faster drug diffusion. Second, increased Sim content results in more drug molecules on or on the particles' surfaces, improving the initial burst release. Similar behaviour was observed by our group reported Meenach *et al.* (2014),¹⁹ where paclitaxel anticancer drug was successfully released from all of the particle systems with the percentage of drug being released increasing with less paclitaxel amount to PL although approximately the same amount of drug was released for all systems mass-wise. Furthermore, the weaker associations between Sim and the phospholipids result in a faster release. These findings highlight the need of adjusting drug-to-phospholipid ratios in dry powder formulations for inhalation in order to obtain uniform and predictable releases.

Conclusion

This systematic study reports for the first time on rationally designed innovative lung surfactant-mimic synthetic DPPC/DPPG phospholipid dry powder particles containing Sim, drug targeting-RhoA/Rho-kinase pathway for targeted pulmonary delivery as high-performing microparticulate/nanoparticulate dry powder inhalation aerosols without the use of non-phospholipid excipients and created by these advanced spray drying conditions in closed-mode. Several different Co-SD nanoformulations as inhalable dry powders were successfully produced as nanoparticles/microparticles with smooth and spherical morphology and showed excellent dispersion performance with all 3 FDA-approved DPI human devices. Excellent biocompatibility on different human lung cells was demonstrated for most of the doses studied. This comprehensive study demonstrates that these innovative Co-SD nanoformulations as inhalable dry powders consisting of Sim and lung surfactant-mimic bionanomaterials can be successfully designed and produced and demonstrates favorable properties as DPIs for the potential new nanomedicine treatment of PH.

Data availability

Data available upon request.

Author contributions

Conceptualization, D. E. B., and H. M. M.; methodology, D. E. B., and H. M. M.; validation, D. E. B., H. M. M.; investigation, D. E. B., and H. M. M.; resources, J. F., S. B., and H. M. M.; data curation, D. E. B., writing—original draft preparation D. E. B., M. F. A., and H. M. M.; writing—review and editing, D. E. B., and H. M. M.; visualization, D. E. B., and H. M. M.; supervision, H. M. M.; project administration, H. M. M.; funding acquisition, H. M. M. All authors have read and agreed to the published version of the manuscript.

Conflicts of interest

The authors declare no conflict of interest.

Acknowledgements

The authors gratefully acknowledge the NIH for 1R01HL137282, R01HL60190, R21AG054766, R21AI13593, and P01HL103453. The authors also gratefully acknowledge the CONACyT (National Council of Science and Technology of Mexico) post-doctoral fellowship awarded to D. E. B. and mentor (HMM). This material is based on research funded by the National Science Foundation under grant number #0619599 and the Arizona Proposition 301: Technology and Research Initiative Fund (A.R.S.15–1648). All SEM images and data were collected in the W.M. Keck Center for Nano-Scale Imaging in the Department of Chemistry and Biochemistry at the University of Arizona with funding from the W. M. Keck Foundation grant. The authors thank Brooke Beam-Massani, Andrei Astachkine of the Imaging Cores Materials Imaging and Characterization Facility supported by the University of Arizona Office of Research, Discovery and Innovation and the X-ray diffraction facility of the Department of Chemistry and Biochemistry at the University of Arizona. The authors gratefully acknowledge the NIH for 1R01HL137282, R01HL60190, R21AG054766, R21AI13593, and P01HL103453. The authors also gratefully acknowledge the CONACyT (National Council of Science and Technology of Mexico) postdoctoral fellowship awarded to D.E.B. and mentor (HMM).

References

- 1 K. S. Awad, J. D. West, V. de Jesus Perez and M. MacLean, Novel signaling pathways in pulmonary arterial hypertension (2015 Grover Conference Series), *Pulm. Circ.*, 2016, **6**(3), 285–294.
- 2 M. M. Hoepfer, V. V. McLaughlin, A. M. Al Dalaan, T. Satoh and N. Galiè, Treatment of pulmonary hypertension, *Lancet Respir. Med.*, 2016, **4**(4), 323–336.
- 3 M. Mandegar, Y.-C. B. Fung, W. Huang, C. V. Remillard, L. J. Rubin and J. X.-J. Yuan, Cellular and molecular mechanisms of pulmonary vascular remodeling: role in the development of pulmonary hypertension, *Microvasc. Res.*, 2004, **68**(2), 75–103.



- 4 G. Loirand and P. Pacaud, The role of Rho protein signaling in hypertension, *Nat. Rev. Cardiol.*, 2010, 7(11), 637.
- 5 H. Courrier, N. Butz and T. Vandamme, Pulmonary drug delivery systems: recent developments and prospects, in *Critical Reviews™ in Therapeutic Drug Carrier Systems* 2002, vol. 19, 4–5.
- 6 S. A. Meenach, F. G. Vogt, K. W. Anderson, J. Z. Hilt, R. C. McGarry and H. M. Mansour, Design, physicochemical characterization, and optimization of organic solution advanced spray-dried inhalable dipalmitoylphosphatidylcholine (DPPC) and dipalmitoylphosphatidylethanolamine poly (ethylene glycol)(DPPE-PEG) microparticles and nanoparticles for targeted respiratory nanomedicine delivery as dry powder inhalation aerosols, *Int. J. Nanomed.*, 2013, 8, 275.
- 7 M. Humbert, E. M. Lau, D. Montani, X. Jaïs, O. Sitbon and G. Simonneau, Advances in therapeutic interventions for patients with pulmonary arterial hypertension, *Circulation*, 2014, 130(24), 2189–2208.
- 8 B. Vaidya and V. Gupta, Novel therapeutic approaches for pulmonary arterial hypertension: Unique molecular targets to site-specific drug delivery, *J. Controlled Release*, 2015, 211, 118–133.
- 9 S. A. Barman, S. Zhu and R. E. White, RhoA/Rho-kinase signaling: a therapeutic target in pulmonary hypertension, *Vasc. Health Risk Manage.*, 2009, 5, 663.
- 10 C. Zhang, J.-M. Wu, M. Liao, J.-I. Wang and C.-J. Xu, The ROCK/GGTase pathway are essential to the proliferation and differentiation of neural stem cells mediated by simvastatin, *J. Mol. Neurosci.*, 2016, 60(4), 474–485.
- 11 J. K. Liao, M. Seto and K. Noma, Rho kinase (ROCK) inhibitors, *J. Cardiovasc. Pharmacol.*, 2007, 50(1), 17.
- 12 K. Sarabandi, P. Gharehbeglou and S. M. Jafari, Spray-drying encapsulation of protein hydrolysates and bioactive peptides: Opportunities and challenges, *Drying Technol.*, 2020, 38(5–6), 577–595.
- 13 B. B. Eedara, W. Alabsi, D. Encinas-Basurto, R. Polt, D. Hayes, S. M. Black and H. M. Mansour, Pulmonary Drug Delivery. In *Organelle and Molecular Targeting*, CRC Press, 2021, pp. 227–278.
- 14 B. B. Eedara, W. Alabsi, D. Encinas-Basurto, R. Polt and H. M. Mansour, Spray-dried inhalable powder formulations of therapeutic proteins and peptides, *AAPS PharmSciTech*, 2021, 22(5), 185.
- 15 A. H. Jobe, Pulmonary surfactant therapy, *N. Engl. J. Med.*, 1993, 328(12), 861–868.
- 16 H. M. Mansour, Y.-S. Rhee, C.-W. Park and P. P. DeLuca, Lipid nanoparticulate drug delivery and nanomedicine, In *Lipids in Nanotechnology*, Elsevier, 2012, pp. 221–268.
- 17 L. Willis, D. Hayes and H. M. Mansour, Therapeutic liposomal dry powder inhalation aerosols for targeted lung delivery, *Lung*, 2012, 190(3), 251–262.
- 18 A. I. Gomez, M. F. Acosta, P. Muralidharan, J. X.-J. Yuan, S. M. Black, Jr, D. Hayes and H. M. Mansour, Therapeutics, Advanced spray dried proliposomes of amphotericin B lung surfactant-mimic phospholipid microparticles/nanoparticles as dry powder inhalers for targeted pulmonary drug delivery, *Pulm. Pharmacol. Ther.*, 2020, 64, 101975.
- 19 S. A. Meenach, K. W. Anderson, J. Z. Hilt, R. C. McGarry and H. M. Mansour, High-performing dry powder inhalers of paclitaxel DPPC/DPPG lung surfactant-mimic multifunctional particles in lung cancer: physicochemical characterization, in vitro aerosol dispersion, and cellular studies, *AAPS PharmSciTech*, 2014, 15(6), 1574–1587.
- 20 W. Alabsi, F. A. Al-Obeidi, R. Polt and H. M. J. P. Mansour, Organic Solution Advanced Spray-Dried Microparticulate/Nanoparticulate Dry Powders of Lactomorphin for Respiratory Delivery: Physicochemical Characterization, In Vitro Aerosol Dispersion, and Cellular Studies, *Pharmaceutics*, 2021, 13(1), 26.
- 21 P. Muralidharan, M. F. Acosta, A. I. Gomez, C. Grijalva, H. Tang, J. X.-J. Yuan and H. M. Mansour, Design and Comprehensive Characterization of Tetramethylpyrazine (TMP) for Targeted Lung Delivery as Inhalation Aerosols in Pulmonary Hypertension (PH): In Vitro Human Lung Cell Culture and In Vivo Efficacy, *Antioxidants*, 2021, 10(3), 427.
- 22 M. F. Acosta, P. Muralidharan, M. D. Abrahamson, C. L. Grijalva, M. Carver, H. Tang, C. Klinger, J. R. Fineman, S. M. Black and H. M. Mansour, Comparison of l-Carnitine and l-Carnitine HCL salt for targeted lung treatment of pulmonary hypertension (PH) as inhalation aerosols: Design, comprehensive characterization, in vitro 2D/3D cell cultures, and in vivo MCT-Rat model of PH, *Pulm. Pharmacol. Ther.*, 2020, 65, 101998.
- 23 H. A. Alhazmi, A. M. Alnami, M. A. Arishi, R. K. Alameer, M. Al Bratty, Z. U. Rehman, S. A. Javed and I. A. J. S. p. Arbab, A fast and validated reversed-phase HPLC method for simultaneous determination of simvastatin, atorvastatin, telmisartan and irbesartan in bulk drugs and tablet formulations, *Sci. Pharm.*, 2018, 86(1), 1.
- 24 The United States Pharmacopoeia and The National Formular, Aerosols, nasal sprays, metered-dose inhalers, and dry powder inhalers monograph, In *USP 29-NF 24: the Official Compendia of Standards 29/24*, ed. Convention, T. U. S. P., The United States Pharmacopoeial Convention, Rockville, MD, 2006, pp. 2617–2636.
- 25 M. F. Acosta, P. Muralidharan, C. L. Grijalva, M. D. Abrahamson, Jr, D. Hayes, J. R. Fineman, S. M. Black and H. M. Mansour, Advanced therapeutic inhalation aerosols of a Nrf2 activator and RhoA/Rho kinase (ROCK) inhibitor for targeted pulmonary drug delivery in pulmonary hypertension: design, characterization, aerosolization, in vitro 2D/3D human lung cell cultures, and in vivo efficacy, *Ther. Adv. Respir. Dis.*, 2021, 15, 1753466621998245.
- 26 W. H. Finlay, *The Mechanics of Inhaled Pharmaceutical Aerosols: an Introduction*, Academic press, 2001.
- 27 H.-J. Lee, J.-H. Kang, H.-G. Lee, D.-W. Kim, Y.-S. Rhee, J.-Y. Kim, E.-S. Park and C.-W. Park, Preparation and physicochemical characterization of spray-dried and jet-milled microparticles containing bosentan hydrate for dry



- powder inhalation aerosols, *Drug Des., Dev. Ther.*, 2016, **10**, 4017.
- 28 P. Russo, M. Stigliani, L. Prota, G. Auriemma, C. Crescenzi, A. Porta and R. P. Aquino, Gentamicin and leucine inhalable powder: what about antipseudomonal activity and permeation through cystic fibrosis mucus?, *Int. J. Pharm.*, 2013, **440**(2), 250–255.
- 29 H. Ren, N. P. Birch and V. Suresh, An optimised human cell culture model for alveolar epithelial transport, *PLoS One*, 2016, **11**(10), e0165225.
- 30 M. A. Chaves and S. C. Pinho, Unpurified soybean lecithins impact on the chemistry of proliposomes and liposome dispersions encapsulating vitamin D3, *Food Biosci.*, 2020, **37**, 100700.
- 31 M. Choudhary, N. Chaurawal, M. A. Barkat and K. Raza, Proliposome-Based Nanostrategies: Challenges and Development as Drug Delivery Systems, *AAPS PharmSciTech*, 2022, **23**(8), 293.
- 32 C. J. Hitzman, W. F. Elmquist, L. W. Wattenberg and T. S. Wiedmann, Development of a respirable, sustained release microcarrier for 5-fluorouracil I: In vitro assessment of liposomes, microspheres, and lipid coated nanoparticles, *J. Pharm. Sci.*, 2006, **95**(5), 1114–1126.
- 33 C.-I. Barbălată, A. S. Porfire, R. Ambrus, M. Mukhtar, Á. Farkas and I. Tomuță, Process development of inhalation powders containing simvastatin loaded liposomes using spray drying technology, *J. Liposome Res.*, 2023, 1–14.
- 34 R. F. Roscigno, T. Vaughn, E. Parsley, T. Hunt, M. A. Eldon and L. J. Rubin, Comparative bioavailability of inhaled treprostinil administered as LIQ861 and Tyvaso® in healthy subjects, *Vasc. Pharmacol.*, 2021, 106840.
- 35 C. Darquenne, Deposition mechanisms, *J. Aerosol Med. Pulm. Drug Delivery*, 2020, **33**(4), 181–185.

